Thermal Challenges in Next Generation Electronic Systems, Joshi & Garimella (eds)

In-plane effective thermal conductivity of plain-weave screen laminates

Jun Xu & R.A. Wirtz
Mechanical Engineering Department/MS 312, University of Nevada Reno, Reno, Nevada, USA

Keywords: thermal conductivity, plain-weave, porosity, screen-laminates.

ABSTRACT: A simple-to-fabricate woven mesh, consisting of bonded laminates of two-dimensional plain-weave conductive screens is described. Geometric equations show that these porous matrices can be fabricated to have a wide range of porosity and specific surface area, β. A heat transfer model is developed. It shows that the laminates can have a highly anisotropic thermal conductivity vector, with in-plane effective thermal conductivities ranging to about 78.5% of base material values. A technique to measure the laminate in-plane effective thermal diffusivity is described. Measurements of the in-plane effective thermal diffusivity of copper plain-weave laminates are used to benchmark the model.

1 NOMENCLATURE

Ay	effective unit cell section area for Y-direction conductivity	$\overline{K}_{fs}$	k_f/k_s
c	specific heat	$\overline{K}ey$	key/k_s
cf	compression factor	Mx, My	mesh numbers along X and Y direction
dx, dy	diameters for the X and Y-direction filaments	$\overline{M}$	My/Mx
$\overline{d}$	dx/dy	Sx, Sy	wire filament lengths
k_{ey}	effective thermal conductivity in Y-direction	t_n	thickness of screen laminates with n layers thickness
k_s	thermal conductivity of base material	R	effective thermal resistance
k_f	thermal conductivity of second phase material	α	thermal diffusivity
		β	surface area-volume ratio
		ε	porosity

2 INTRODUCTION

A thermally conductive, open cell porous matrix such as an unconsolidated bed of small particles, or foamed metal such as foamed aluminum, make excellent heat exchanger surfaces due to their large surface area-to-volume property, β. Also, when used as a fill material, these matrices are effective solid composite conductivity enhancers. However, due to high porosity (ε) coupled with the tortuosity effect, the effective thermal conductivity of these materials, k_e is relatively small, so that much of the gain in performance obtained by having a large β is lost by having a relatively small k_e. Typical values of k_e in spherical particle packed beds are 10% - 15% of the particle ther-

mal conductivity, k_s [Kaviany, 1995]. Commercially available metal foam such as aluminum foam, has an effective thermal conductivity that ranges from 2% to 6% of the base metal value [Ashby et al, 2000].

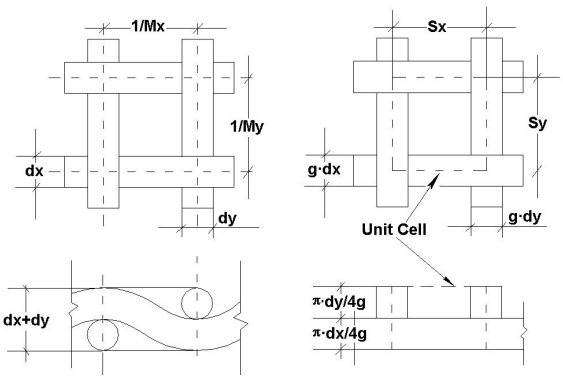

Fig. 1 Plain-weave unit cell.

An anisotropic porous matrix having a large surface area to volume ratio and high effective thermal conductivity in a particular direction will result in a very effective heat exchange device. In this paper, we show that stacked laminates of conductive screening can be configured to have these characteristics. Such a porous matrix can be incorporated into the design of a flow-through module or cold plate heat exchanger, resulting in a compact, high-flux device with reasonable pressure-drop characteristics [Park et al, 2002]. Furthermore, these laminates, when incorporated into a polymer-based composite sandwich structure, are promising conductivity enhancers [Zhao et al, 2002].

The earliest model for the effective thermal conductivity of a porous material is attributed to Rayleigh [1892, as referenced in Alexander, 1972]. The model assumes that the porous material is isotropic. More recently, Alexander [1972], Koh and Fortini [1973] and Chang [1990] have reported models and empirical correlations specifically directed at the cross-plane effective thermal conductivity component of screen material. We have found no reference in the technical literature for the in-plane component of the effective thermal conductivity.

3 PHYSICAL MODEL

Figure 1 summarizes the development of the thermal/physical model of a plain-weave screen. The left segment of the figure shows plan and edge views of a section of screen. Serpentine wire filaments have diameter dx and dy, and corresponding mesh numbers Mx and My. The wire filament pitch in the x- and y-directions are $Mx^{-1} = wx + dy$ and $My^{-1} = wy + dx$, respectively. In the absence of crimping, the screen has thickness $t_1 = dx + dy$. Filament lengths are [Luo and Mitra, 1999]

$$Sx = \frac{1}{Mx}\left[1 + 9.6\left(\frac{dy \cdot Mx}{4}\right)^2 - 49.2\left(\frac{dy \cdot Mx}{4}\right)^4\right] \tag{1}$$

$$Sy = \frac{1}{My}\left[1 + 9.6\left(\frac{dx \cdot My}{4}\right)^2 - 49.2\left(\frac{dx \cdot My}{4}\right)^4\right] \tag{2}$$

Following Chang [1990], we transform the section of screen into the layered, rectangular cross section segment shown in the right segment of the figure. Each rectangular wire filament has thick-

ness $\pi d/4g$ and width gd so that the cross section area of each filament is $\pi d^2/4$. The geometric index, g is a measure of the contact between wire filaments at intersections.

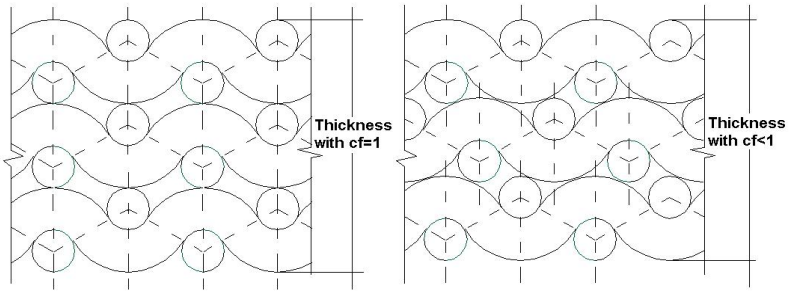

Fig. 2 Screen stacking configurations.

Figure 2 shows two possible arrangements of stacked plain-weave screens. The left hand view shows the situation where successive wire filaments are aligned so that the thickness of a laminate consisting of n screens is $t_n = n(dx+dy)$. The right element of the figure shows the situation where successive wire filaments are not necessarily in line so there is some interleaving of wire filaments when the screens are stacked. In this case, the thickness of the laminate is $t_n = n \cdot c_f (dx+dy)$ where c_f is the compression factor. The magnitude of the compression factor depends on the weave pattern, mesh numbers and wire filament diameters of the screen, and the stacking arrangement of the screen layers. If we restrict our attention to screens with $t_1 = dx+dy$, then $cf \le 1$.

Consideration of Figs. 1 and 2 leads to expressions for the porosity, ε and specific surface area, β of plain-weave screen laminates.

$$cf \cdot (1-\varepsilon) = \frac{\left(\pi \cdot dy^2 Sy + \pi \cdot dx^2 Sx\right) \cdot Mx \cdot My}{4(dx+dy)} \tag{3}$$

where $cf(1-\varepsilon)$ is the reduced "metal" fraction.

$$\beta = SF(1-\varepsilon) \tag{4}$$

SF in Eq. (4) is the shape factor for the particular weave pattern and stacking arrangement

$$SF = \frac{4(dy \cdot Sy \cdot Mx + dx \cdot Sx \cdot My)}{dy^2 \cdot Sy \cdot Mx + dx^2 \cdot Sx \cdot My} \tag{5}$$

If we introduce mesh number and wire filament diameter ratios $\overline{M} = My/Mx$ and $\overline{d} = dx/dy$, then it can be shown [Xu, 2001] that the reduced metal fraction is a function of $(Mxdy, \overline{M}, \overline{d})$ and β is a function of $(cf(1-\varepsilon), \overline{M}, \overline{d})$.

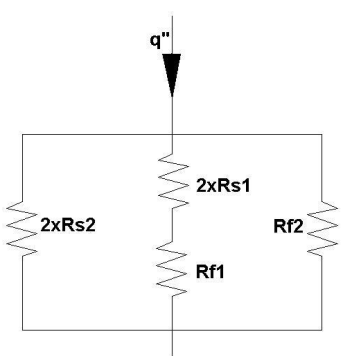

Fig. 3 Thermal circuit.

The in-plane effective thermal conductivity in the y-direction may be determined by considering the thermal circuit for conduction across the transformed unit cell, shown in Fig. 3. The figure shows three heat-flow paths: R_{s2} is the thermal resistance for conduction along the axis of the y-wire filaments; R_{s1} is the thermal resistance across x-wire filaments; R_{f1} is the thermal resistance to conduction in the y-direction, across the intervening "fluid" lying between x-wire filaments; and, R_{f2} in the thermal resistance of the fluid slab that lays between the y-wire filaments. These resistances are given as

$$R_{s1} = \frac{2g^2 \cdot dx}{\pi \cdot Ks \cdot dx \cdot Sx} \tag{6}$$

$$R_{s2} = \frac{8Sy}{\pi \cdot K_s \cdot dy^2} \tag{7}$$

$$R_{f1} = \frac{4g \cdot Sy(My, dx) - 4g^2 dx}{\pi \cdot K_f \cdot dx \cdot Sx} \tag{8}$$

$$R_{f2} = \frac{4g \cdot Sy}{\pi \cdot K_f \cdot (Sx - g \cdot dy) \cdot dy} \tag{9}$$

We further require that the volume of wire filaments be preserved across the geometric transformation shown in Fig. 1. Then $g = \pi / 4 \cdot cf$

If we define the effective thermal conductivity in the y-direction as $ke_y = qMy^{-1} / \Delta T$, then

$$cf \cdot \overline{K}_{ey} = \frac{1}{(\overline{d}+1)}\left[\frac{160\pi Mxdy \cdot (\overline{K}_{fs}-1) + C \cdot \overline{K}_{fs} \cdot cf^{-1}}{D \cdot \overline{K}_{fs}} + \frac{C \cdot \overline{d} \cdot \overline{K}_{fs}}{160\pi \cdot \overline{d} \cdot \overline{M} \cdot Mxdy(1-\overline{K}_{fs}) + C \cdot cf^{-1}}\right] \tag{10}$$

$$C = 123(Mx \cdot dy)^4 - 384(Mx \cdot dy)^2 - 640 \tag{11}$$

$$D = 123(My \cdot dx)^4 - 384(My \cdot dx)^2 - 640 \tag{12}$$

where $\overline{Ke}_y = ke_y / k_s$ and $\overline{K}_{fs} = k_f / k_s$ are the dimensionless effective conductivity and "fluid" conductivity, respectively.

Since most available commercial woven mesh products are isotropic structures, i.e *dx=dy=d and Mx=My=M*, the above general results can be simplified.

$$cf\left[1-\varepsilon(iso)\right] = -3.906\times10^{-4}\pi \cdot C \cdot Md \tag{13}$$

$$\beta(iso) = 4(1-\varepsilon)/d \tag{14}$$

$$cf \cdot \overline{K}_e(iso) = \frac{1}{2}\left[\frac{160\pi \cdot Md \cdot (\overline{K}_{fs}-1) + C \cdot \overline{K}_{fs} \cdot cf^{-1}}{C} + \frac{C \cdot \overline{K}_{fs}}{160\pi \cdot Md(1-\overline{K}_{fs}) + C \cdot cf^{-1}}\right] \tag{15}$$

Equation 13 shows that the reduced "metal fraction", $cf(1-\varepsilon)$ is solely a function of the *Md*-product of the mesh. We note that $Md \to 1$ designates a "tightly" woven screen. In actuality, there is a physical limit on the magnitude of *Md*. For isotropic plain-weave screens where the thickness is limited to $t_1 = 2d$, $Md_{2d}(\max) = 1/\sqrt{3} = 0.577$ so that the porosity is limited such that $0 < cf(1-\varepsilon) < 0.534$.

Equation (14) shows that the specific surface area, β follows the functional form of other porous media, with $SF = 4/d$. By contrast, $SF(spheres) = 6/d_s$ for an unconsolidated bed of spherical particles. Note, ε(spheres) is generally limited to a constant value of about 0.38.

Finally, Eq. (15) shows that the effective conductivity $\overline{Ke}_y(iso)$ is solely a function of $\overline{K}_{fs}$ and *Md*. It can be shown [Xu, 2001] that $\overline{Ke}_y(iso)$ is solely a function of $\overline{K}_{fs}$ and ε.

Figure 4 plots the reduced metal fraction as a function of *Mxdy*. The case for an isotropic screen laminate is shown as a solid line. This case always produces screen laminates having the highest

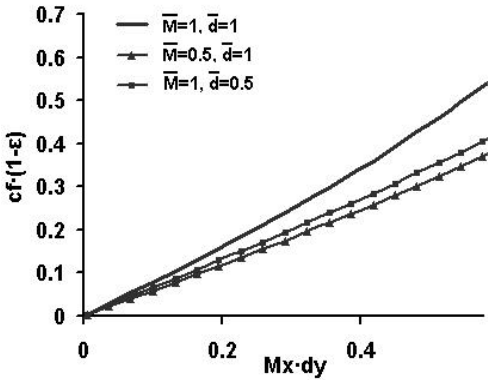

Fig. 4 Screen laminate reduced metal fraction.

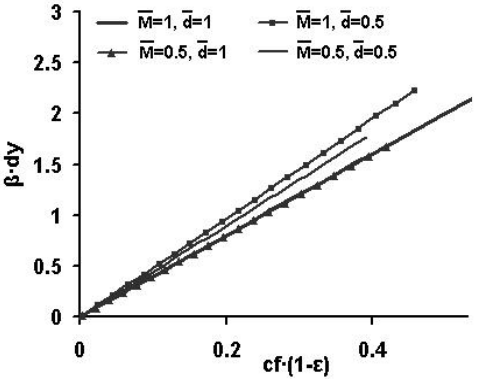

Fig. 5 Screen laminate specific surface area.

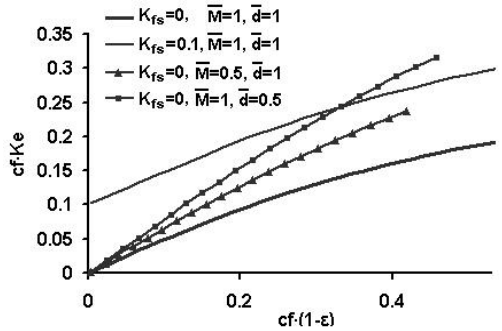

Fig. 6 Screen laminate conductivity.

metal fraction (lowest porosity). The reduced metal fraction for two anisotropic plain-weave laminate cases ($\overline{M}<1$, $\overline{d}<1$) are also shown in the figure.

Figure 5 plots βdy as a function of reduced metal fraction. The case for an isotropic screen laminate is shown as a bold solid line. The shape factor for this condition is SF = 4 (the slope of the plotted line). This is true for all conditions where $\overline{d}=1$. The case $\overline{M}=0.5$, $\overline{d}=1$ is shown superimposed on the isotropic case. All conditions with $\overline{M}<1$, $\overline{d}<1$ lead to larger values of βdy at fixed $Mxdy$. Therefore, the condition $\overline{d}=1$ always produces the smallest specific surface area.

Figure 6 plots the reduced effective conductivity as a function of reduced metal fraction. The case for an isotropic screen laminate with $\overline{K}_{fs}=0$ is shown as a bold solid line. An additional case, isotropic screen laminate with $\overline{K}_{fs}=0.1$ is also shown (solid line). Under these conditions, the effective conductivity is shifted upward approximately proportional to the value of $\overline{K}_{fs}$. In many applications where the second phase material is a hydrocarbon with the first phase a "good" conductor, $\overline{K}_{fs}<0.005$.

Two additional, anisotropic screen laminate cases are shown in the figure. Cases with $\overline{M}<1$ or $\overline{d}<1$ always produce effective conductivities that are greater than obtained with isotropic plain-weaves.

It is easy to find the maximum possible value of $\overline{Key}$. When the $Mxdy\to 1$, $\overline{M}\to 0$ and $\overline{d}\to 0$, then, Eq. (10) gives,

$$Ke_y(\max)=\frac{(1-\pi)k_{fs}}{4}+\frac{\pi}{4} \tag{16}$$

Therefore, $Ke_y(\max)$ can be greater than 0.785.

4 MODEL VERIFICATION WITH EXPERIMENT

4.1 *Measurement of thermal diffusivity*

Consider a uniform cross section, long and slender test article with well-insulated periphery, as shown in Fig. 7. The test article is initially at a uniform temperature, T_i when a time-varying heat flux is applied to one end. We measure the temperature response at three locations, as shown in the figure. Assume constant thermophysical properties and one-dimensional transient conduction in the domain between points 1 and 3. The temperature response at point 2 will be given as

$$\Delta T_2(time) = fct(\Delta T_1(time), \Delta T_3(time); \alpha, \Delta y_1, \Delta y_2) \tag{17}$$

The temperature response at point 1 describes the heat input to the test domain; that at point 3 describes the heat outflow from the test domain. Then, the temperature response at point 2 can be used to determine the thermal diffusivity, α.

The test rig consists of a radiant heat source and shutter mechanism, and well-insulated screen laminate test articles that are approximately 200mm long. Temperatures at points 1, 2 and 3 are sensed with 0.25mm diameter Type T thermocouples that are soldered to the test article. Measurement points are located with an accuracy of ±0.1mm. Temperatures are recorded at a rate of 10 – 20 samples per second, with an accuracy of approximately ±0.2°C.

Three bar-shaped oxygen-free copper test articles (Alloy C10100, $\alpha = 11.1x10^{-5}m^2/s$) were tested. Each test was repeated six times. The mean measured thermal diffusivity for each of the test articles was $11.76x10^{-5}m^2/s$, $11.62x10^{-5}m^2/s$ and $11.72x10^{-5}m^2/s$, giving an overall average value of $11.7x10^{-5}m^2/s$. The 95% confidence interval for all 18 measurements (2σ about mean values) is $0.7x10^{-5}m^2/s$ and the implied offset error, based on the handbook value of thermal diffusivity of alloy C10100, is +5.2%.

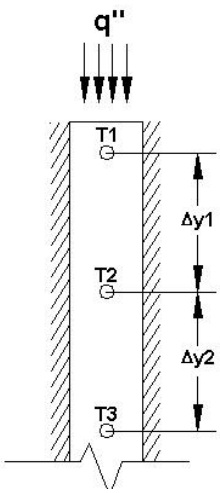

Fig. 7 Test configuration.

4.2 *Screen laminates test articles*

Isotropic, plain-weave copper screens are stacked and bonded together (using 95/5 Sn/Pb solder) to form the screen laminates. Various screen laminate samples were fabricated with this method: the mesh numbers range from $6.3cm^{-1}$ $(16inch^{-1})$ to $15.75cm^{-1}$ $(40inch^{-1})$, the bare copper wire filament diameter ranges from *0.28mm* to *0.46mm*, and the number of layers ranges from 3 to 10. Measured compression factors range from 0.70 to 1.00. Figure 8 shows a typical copper plain-weave screen-laminate. The wire filaments have an effective diameter of *0.48mm*, and the mesh number is $6.3cm^{-1}$ $(16inch^{-1})$. The sample has $\varepsilon = 0.689$, $\beta = 2592m^{-1}$.

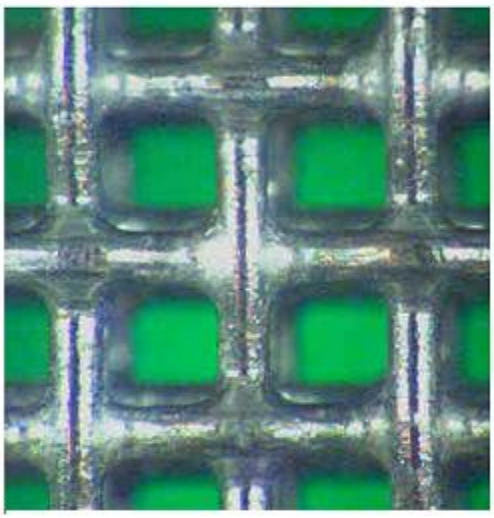

Fig. 8. Bonded screen laminate.

Twenty (20) test articles of the above mentioned fabricated isotropic screen laminates specimens are tested. In the calculation, the effective density/specific heat product, ρc of the screen laminate is calculated based on the measured weight ratios of copper and solder material in the composites. The copper wire properties are: $\rho = 8940$ kg/m^3, $c = 393.5$ J/(kg·K, $k_s = 400$ W/mK). The Sn-Pb solder material's properties are: $\rho = 7317$kg/m^3, $c = 230.0$J/kg·K, $k_s = 56$ W/mK. As

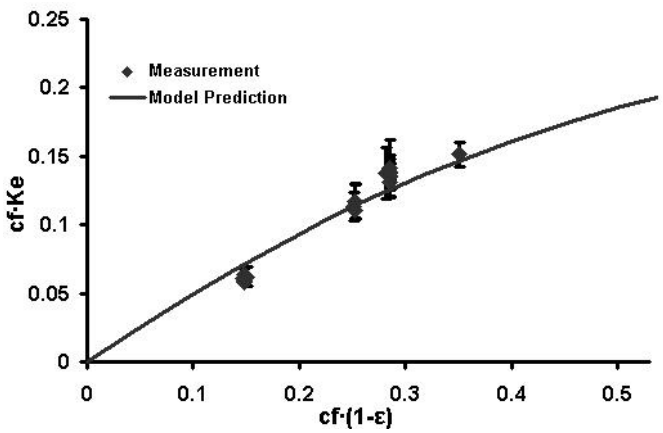

Fig. 9 Benchmark measurements of ke_y in air.

different specimens have different weight ratios of copper and solder material, so the calculated effective densities for the laminates range from 8694kg/m^3 to 8796kg/m^3, the specific heats range from 369.1J/kg·K to 379.0J/kg·K and, the thermal conductivity range from 349.7 W/mK to 371.1 W/mK. The thermal conductivity of air at temperature of 323K, 0.0278W/m·K is used.

4.3 *Test results.*

The average test result of reduced dimensionless in-plane equivalent conductivity for each specimen is shown with 2σ error bars in Figure 9. Each data point shown represents six or more test runs of the same sample. The model prediction for the isotropic plain-weave screen laminate saturated with air is also shown in the figure. It shows that the prediction of the present model is within 10% of all of the measurements. With consideration of the non-uniform solder layer's thickness on the filaments, and non-uniform properties of the high porosity screens, the prediction of the present model is quite accurate.

5 CONCLUSION

Simple porous media structures can be fabricated from conductive screening. The resulting structures can be configured to have a wide range of porosity, specific surface area and in-plane effective thermal conductivity which could be up to 23% and 78% of the filament material's conductivity for isotropic and anisotropic plain-weave screen laminates, respectively. The in-plane effective thermal conductivity of screen laminates, in particular for anisotropic screen laminates is much greater than that can be achieved with other porous media configurations. The material can be configured to have highly anisotropic thermal properties while at the same time high porosity is maintained.

The simple universal model for effective in-plane thermal conductivity and porosity has been verified with benchmark experiments. A technique for thermal conductivity (diffusivity) is set up and calibrated.

6 ACKNOWLEDGEMENT/DISCLAIMER

The Ballistic Missile Defense Organization through the Air Force Office of Scientific Research, USAF, sponsors this work under contract number F49620-99-0286. The views and conclusions contained herein are those of the authors and should not be interpreted as necessarily representing the official policies or endorsements, either expressed or implied, of the Ballistic Missile Defense Organization, the Air force Office of Scientific Research, or the U.S. Government..

REFERENCES

Ashby, M., Evans, A., Fleck, N., Gibson, L., Hutchinson, J. & Wadley, H. 2000. Metal Foams, A Design Guide. Butterworth Heinemann.

Alexander, E. G. Jr. 1972. Structure-Property Relationships in Heat Pipe Wicking Materials. *Ph.D. thesis, Department of Chemical Engineering, North Carolina State University*, Raleigh, NC

Chang, Woo Soon. 1990. Porosity and Effective Thermal Conductivity of Wire Screens. *Journal of Heat Transfer, Feb. 1990, Vol. 112*.

Kaviany, M. 1995. *Principals of Heat Transfer in Porous Media*, *2-nd ed*., Springer.

Koh, J. C. Y. & Fortni, A. 1973. Prediction of thermal conductivity and electrical resistivity of porous metallic materials. *Int. J. Heat Mass Transfer, Vol. 16, pp. 2013-2021*

Luo, S.Y. & Mitra, A. 1999. Finite Elastic Behavior of Flexible Fabric Composite Under Biaxial Loading. *Journal of Applied Mechanics, Vol. 66, pp 631-638*.

Park, J-Wook, Ruch, D. & Wirtz, R.A. 2002 Thermal/Fluid Characteristics of Plain-Weave Laminates as Heat Exchanger Surfaces. *Accepted, 40-th AIAA Aerospace Sciences Meeting and Exhibit*, Reno, NV

Xu, J. 2001. In-Plane Effective Thermal Conductivity of Plain Weave Screen Laminates. *M.S. Thesis, Mechanical Engineering Department, University of Nevada, Reno*, NV 89557, USA.

Zhao, T-W, Narla, V, Fuchs, A., Jiang, Y., & Wirtz, R. A. 2002. Thermal and Mechanical Properties of Woven Mesh Thermal Energy Storage Composites. *pending, AIAA/ASME Thermophysics and Heat Transfer Conf.*